

Turbulence, Heat and Mass Transfer 8

Proceedings of the Eight International Symposium
On Turbulence, Heat and Mass Transfer
Sarajevo, Bosnia and Herzegovina, 15-18 September, 2015

Edited by

K. HANJALIĆ

*Delft University of Technology, The Netherlands, and
Novosibirsk State University, Russia*

T. MIYAUCHI

*Tokyo Institute of Technology, and
Meiji University, Japan*

D. BORELLO

Sapienza University of Rome, Italy

M. HADŽIABDIĆ

International University of Sarajevo, Bosnia and Herzegovina

P. VENTURINI

Sapienza University of Rome, Italy



Begell House Inc.
New York, Wallingford (UK)

**International
Centre for Heat
and Mass Transfer**



Large eddy simulation of MHD turbulence decay at different magnetic Reynolds number

D. B. Zhakebayev¹, A. K. Khikmetov¹, A. U. Abdibekova¹

¹*Department of Mathematical and computer modelling, Kazakh National University named after al-Farabi, al-Farabi 71, 050012 Almaty, Kazakhstan, daurjaz@mail.ru*

Abstract – We consider the numerical simulation of homogeneous magnetohydrodynamic turbulence decay depending on magnetic Reynolds number based on large eddy simulation. To close magnetohydrodynamic equation system the modified dynamic model is used and calculated at each time steps. Depending on the different magnetic Reynolds number the variation of the kinetic and magnetic energies of turbulence with time, and depending on the time the micro- and macro-scale turbulence were obtained.

1. Introduction

In spite of the large number of publications in this field, the study of the homogeneous magnetohydrodynamic (MHD) turbulence decay process is a relevant task for researchers of several generations. The influence of the magnetic field on conducting fluids is studied in different scientific fields and applied in engineering and technology. Therefore, investigations of the MHD turbulence decay is an important problem for astrophysical and geophysical phenomena formation, MHD generators, plasma accelerators and engines [1-4].

The research problems of the magnetic field influence on electrically conducting fluids are split in three types:

1. Study of MHD turbulence at a constant value of the magnetic field.
2. Study the magnetic field self-excitation at a given velocity of flow.
3. Study of the magnetic field self-excitation and motion of a conducting fluid considering, at the same time, the acting forces.

This work is devoted to the study of the magnetic field self-excitation and to the motion of a conducting fluid, at the same time taking into account the acting forces. Although a lot of authors have dedicated their works to this field it is still relevant today. The results of study this problem are presented in [5] the influence of external magnetic field on the decay of MHD turbulent flow at the low magnetic Reynolds number by LES and DNS methods, and demonstrated that magnetic field in the start begins to decay when exposed to the total kinetic energy. This effect is consistent with Joule dissipation. LES method has shown excellent result in adaptation Smagorinsky dynamic model to the flow and the applied magnetic field through the dynamic procedure. A similar picture of the decay was not reported by the authors, Knaepen and Moin, because their main objective was the evaluation of the model adequacy for the LES and DNS methods.

Later, a resembling problems for anisotropy of MHD turbulence were researched by [6, 7], which reflected the change in the turbulence statistical parameters as a result of an imposed magnetic field influence. The contribution of these scientists in this area of expertise is determined by proving that the behavior of two- and three-dimensional structures varies

THMT '15

Proceedings of the International Symposium

Turbulence, Heat and Mass Transfer 8

Sarajevo, Bosnia and Herzegovina, September 15-18 2015

Edited by

**K. Hanjalić, T. Miyauchi, D. Borello,
M. Hadžiabdić and P. Venturini**



International Centre for
Heat and Mass Transfer

Begell House Inc.
ISBN 978-1-56700-428-8
ISSN 2377-4169



Organizing Committee

K. Hanjalić, Chairman
T. Miyauchi, Co-Chairman
D. Borello, Symposium Secretary
M. Hadžiabdić, Organizing Secretary
J.-P. Bonnet, *University of Poitiers, France*
E. Džaferović, *University of Sarajevo, BH*
E. Ganić, *Sarajevo School of Sci. Techn. BH*
T.B. Gatski, *Old Dominion University, USA*
S.S. Girimaji, *Texas A&M University, USA*
S. Jakirlić, *Darmstadt Univ. Techn., Germany*
S. Kenjereš, *Delft Univ. of Technology, NL*
B.E. Launder, *University of Manchester, UK*
D. Laurence, *Electricité de France*
D. Markovich, *ITP SB RAS/NSU, Russia*
I. Marusic, *University of Melbourne, Australia*
Y. Nagano, *Nagoya Inst. of Technology, Japan*
A. Pollard, *Queen's University, Canada*
F. Rispoli, *'Sapienza' University, Rome, Italy*
M. Tanahashi, *Tokyo Inst. of Techn., Japan*

Scientific Advisory Committee

R. Amano, *USA*
H.I. Andersson, *Norway*
V. Armenio, *Italy*
B. Basara, *Austria*
S. Benhamadouche, *France*
D. Bergstrom, *Canada*
B.J. Boersma, *NL*
C.M. Casciola, *Italy*
I. Castro, *UK*
H. Choi, *Korea*
A. Corsini, *Italy*
D. Čokljat, *UK*
T.J. Craft, *UK*
L. Davidson, *Sweden*
C. Dopazo, *Spain*
S. Drobniak, *Poland*
S.E. Elghobashi, *USA*
M. Fairweather, *UK*
S. Frolov, *Russia*
S. Fu, *China*
Y. Hagiwara, *Japan*
H. Hattori, *Japan*
E. Hawkes, *Australia*
G. Hetsroni[†], *Israel*
R.J.A. Howard, *France*
J. Janicka, *Germany*
T. Kajishima, *Japan*
J. Klewicki, *Australia/USA*
S. Komori, *Japan*
S. Lardeau, *UK*
R. Manceau, *France*
E. Mastorakos, *UK*
S. Obi, *Japan*
S-H Peng, *Sweden*
J.C. Pereira, *Portugal*
M. Reeks, *UK*
M. Van Reeuwijk, *UK*
D.J.E.M. Roekaerts, *NL*
G.P. Romano, *Italy*
E. Serre, *France*
J. Sesterhenn, *Germany*
D.Ph. Sikovsky, *Russia*
A.P. Silva Freire, *Brazil*
A. Soldati, *Italy*
M. Strelets, *Russia*
K. Suga, *Japan*
H.J. Sung, *Korea*
J. Szmyd, *Poland*
A. Tomboulides, *Greece*
P. Tucker, *UK*
L. Vervisch, *France*
S. Wallin, *Sweden*
H. Yoshida, *Japan*
Z. Zhang, *China*

Patronage/Sponsors/Donators

Academy of Sciences and Arts of BH
Mayor of City of Sarajevo, *BH*
The University of Sarajevo, *BH*
International University of Sarajevo, *BH*
Delft University of Technology, *The Netherlands*
Sapienza University of Rome, *Italy*
Tokyo Institute of Technology, *Japan*
Electricité de France – R&D, *France*
AVL-List GmbH, *Austria*

Viessmann, *Croatia*
UNDP, *BH*
HVAC, *BH*
Mountain, *BH*
Interklima, *BH*
Weishaupt, *BH*
AluCo & Co. *BH*
Energy Design, *BH*
Bosna-S Eng., Oil&Gas, *BH*



substantially.

In addition, investigation of pseudospectral direct numerical simulation, with up to 1024^3 nodes, three-dimensional incompressible MHD turbulence, and with no mean magnetic field in a high resolution was detailed in [8]. The study was carried out considering various statistical properties of both decreasing and statistically steady MHD turbulence on the magnetic Prandtl number Pm taken over a wide range of $0.01 \leq Pm \leq 10$. Turbulent characteristics were obtained at a constant magnetic viscosity for different values of kinetic viscosity.

Therefore, there is a need to examine this process over a wide range of Re_m numbers to determine the pattern of the magnetic field impact on the turbulence decay for fluids that vary in their electrical conductivity. It is known, when the Re_m number is small, the impact of the magnetic field on the kinetic energy is significant because the turbulence degeneration is faster than in the case of a large Re_m number when the impact is negligible, and the process is similar to the case of an isotropic turbulence. This effect also demonstrates the process dynamics with various Alfvén numbers. This work is devoted to the study of the magnetic field self-excitation and to the motion of a conducting fluid, at the same time taking into account the acting forces. The idea is to specify initial conditions in the phase space for a velocity and magnetic fields, which satisfy the condition of continuity. The given initial condition with the phase space is translated into physical space using a Fourier transform. The obtained velocity and magnetic fields are used as initial conditions for the filtered MHD equations. Further, the unsteady three-dimensional MHD equation is solved to simulate the homogeneous MHD turbulence decay.

2. Problem formulation

The problem is numerically modelled by solving the non-stationary filtered magnetic hydrodynamics equations in conjunction with the continuity equation in the Cartesian coordinate system in a non-dimensional form:

$$\left\{ \begin{array}{l} \frac{\partial \bar{u}_i}{\partial t} + \frac{\partial (\bar{u}_i \bar{u}_j)}{\partial x_j} = -\frac{\partial \bar{p}}{\partial x_i} + \frac{1}{Re} \left(\frac{\partial^2 \bar{u}_i}{\partial x_j^2} \right) - \frac{\partial \tau_{ij}^u}{\partial x_j} + A \frac{\partial}{\partial x_j} (\bar{H}_i \bar{H}_j), \\ \frac{\partial \bar{u}_i}{\partial x_i} = 0, \\ \frac{\partial \bar{H}_i}{\partial t} + \frac{\partial}{\partial x_j} (\bar{u}_j \bar{H}_i - \bar{H}_j \bar{u}_i) = \frac{1}{Re_m} \frac{\partial^2 \bar{H}_i}{\partial x_j^2} - \frac{\partial \tau_{ij}^H}{\partial x_j}, \\ \frac{\partial \bar{H}_i}{\partial x_i} = 0, \\ \text{where } \tau_{i,j}^H = \left(\overline{(u_i u_j)} - (\bar{u}_i \bar{u}_j) \right) - \left(\overline{(H_i H_j)} - (\bar{H}_i \bar{H}_j) \right), \\ \tau_{i,j}^u = \left(\overline{(u_i H_j)} - (\bar{u}_i \bar{H}_j) \right) - \left(\overline{(H_i u_j)} - (\bar{H}_i \bar{u}_j) \right). \end{array} \right. \quad (1)$$

where \bar{u}_i ($i = 1, 2, 3$) are the velocity components, $\bar{H}_1, \bar{H}_2, \bar{H}_3$ are the magnetic field strength components, $A = H^2 / (4\pi\rho V^2) = \Pi / Re_m^2$ is the Alfvén number, H is the

characteristic value of the magnetic field strength, V is the typical velocity, $\Pi = (V_A L / \nu_m)^2$ is a dimensionless value (on which the value Π depends in the equation for \bar{H}_i). If $\Pi \ll 1$, then $\partial \bar{H}_i / \partial t = 0$. The publication [9] discusses in detail the physics of the phenomena related to the ability to disregard the summand $V_A = H / \sqrt{4\pi\rho}$ is the Alfven velocity, $\bar{p} = p + \bar{H}^2 A / 2$ is the full pressure, t is the time, $\text{Re} = LV / \nu$ is the Reynolds number, $\text{Re}_m = LV / \nu_m$ is the magnetic Reynolds number, L is the typical length, ν is the kinematic viscosity coefficient, ν_m is the magnetic viscosity coefficient, ρ is the density of an electrically conducting incompressible fluid, and τ_{ij}^u, τ_{ij}^H are the subgrid - scale tensors responsible for small-scale structures to be modelled.

Periodic boundary conditions are selected at all boundaries of the considered area of the velocity components and magnetic field strength. The initial values for each velocity component and strength are defined in the form of a function, which depends on the wave numbers in the phase space [10].

3. Method to calculate the small-scale turbulence coefficient.

Along with the accepted calculated grid, a grid with twice the size of the cells along each axis is used. The large grid number cell is indicated as p, g, r (p, g, r are the axes numbered x_1, x_2, x_3 respectively), $p = 1, 2, 3, \dots, N_1/2$, $g = 1, 2, 3, \dots, N_2/2$, and $r = 1, 2, 3, \dots, N_3/2$. The cell with the number α along the axis x_1 includes the cells of the initial grid with numbers $n = 2p - 1$ and $n = 2p$, where n varies within the range from 1 to N_1 . Similar to the number g , for x_2 cells with numbers $m = 2g - 1$ and $m = 2g$, $q = 2r - 1$ and $q = 2r$ were determined. Therefore, one cell p, g, r of a large grid is the same as eight cells of the initial grid.

The average values u_1^2, u_2^2, u_3^2 for the total volume of the calculated area of the liquid flow are marked as $\langle u_1^2 \rangle, \langle u_2^2 \rangle, \langle u_3^2 \rangle$. These values can be calculated using smaller and larger calculation grids:

$$\langle u_i^2 \rangle = \frac{1}{N_1 N_2 N_3} \cdot \sum_{n=1}^{N_1} \sum_{m=1}^{N_2} \sum_{q=1}^{N_3} [(\bar{u}_i)^2 + (u_i')^2] \quad (2)$$

where $(\bar{u}_i)^2 = \bar{u}_i \bar{u}_i$ and $(u_i')^2 = \overline{u_i' \cdot u_i'}$.

The subgrid-scale tensor for smaller cells is

$$\tau_{ij} = \overline{u_i' u_j'} = -2C_S \cdot \Delta_s^2 \cdot (2 \cdot \bar{S}_{ij}^s \cdot \bar{S}_{ij}^s)^{\frac{1}{2}} \cdot \bar{S}_{ij}^s \quad (3)$$

where $\Delta_s = (\Delta_i \Delta_j \Delta_k)^{1/3}$ is the width grid filter of the small cell.

The deformation velocity calculated in smaller cells is $\bar{S}_{ij}^s = \frac{1}{2} \left(\frac{\partial \bar{u}_i^s}{\partial x_j} + \frac{\partial \bar{u}_j^s}{\partial x_i} \right)$,

where $n = \overline{1, N_1}$, $m = \overline{1, N_2}$, $q = \overline{1, N_3}$.

By substituting expression (3) into Eq. (2), we can obtain the average velocity value calculated in the smaller cells:

$$\langle u_i^2 \rangle^s = \frac{1}{N_1 N_2 N_3} \cdot \sum_{n=1}^{N_1} \sum_{m=1}^{N_2} \sum_{q=1}^{N_3} \left[(\bar{u}_i^s)^2 - 2 \cdot C_S \cdot \Delta_s^2 \cdot (2 \cdot S_{ij}^s \cdot S_{ij}^s)^{\frac{1}{2}} S_{ij}^s \right] \quad (4)$$

The average velocity calculated in the larger cells is

$$\langle u_i^2 \rangle^l = \frac{8}{N_1 N_2 N_3} \cdot \sum_{p=1}^{N_1/2} \sum_{g=1}^{N_2/2} \sum_{r=1}^{N_3/2} \left[(\bar{u}_i^l)^2 - 2 \cdot C_S \cdot \Delta_l^2 \cdot (2 \cdot S_{ij}^l \cdot S_{ij}^l)^{\frac{1}{2}} S_{ij}^l \right] \quad (5)$$

where $\Delta_l = (\Delta_i \Delta_j \Delta_k)^{1/3}$ is the width grid filter of the large cell, $\Delta_l = 2\Delta_s$.

The deformation velocity calculated in the larger cells is

$$S_{ij}^l = \frac{1}{2} \left(\frac{\partial \bar{u}_i^l}{\partial x_j} + \frac{\partial \bar{u}_j^l}{\partial x_i} \right),$$

where $p = 1, 2, 3, \dots, N_1/2$, $g = 1, 2, 3, \dots, N_2/2$, $r = 1, 2, 3, \dots, N_3/2$.

$$\bar{u}_i^l(p, g, r) = \frac{1}{8} \left[\begin{aligned} & \bar{u}_i^s(2p-1, 2g-1, 2r-1) + \bar{u}_i^s(2p-1, 2g, 2r-1) + \bar{u}_i^s(2p-1, 2g, 2r) + \\ & \bar{u}_i^s(2p-1, 2g-1, 2r) + \bar{u}_i^s(2p, 2g-1, 2r-1) + \bar{u}_i^s(2p, 2g, 2r-1) + \\ & \bar{u}_i^s(2p, 2g, 2r) + \bar{u}_i^s(2p, 2g-1, 2r) \end{aligned} \right];$$

We introduce the following notation:

$$F^u = \left(\langle u_1^2 \rangle^s + \langle u_2^2 \rangle^s + \langle u_3^2 \rangle^s - \langle u_1^2 \rangle^l - \langle u_2^2 \rangle^l - \langle u_3^2 \rangle^l \right)^2$$

From equations (4) and (5) we can conclude that

$$F^u = (Z^u - Y^u \cdot C_S)^2$$

where

$$\begin{aligned} Z^u &= \frac{1}{N_1 N_2 N_3} \cdot \sum_{n=1}^{N_1} \sum_{m=1}^{N_2} \sum_{q=1}^{N_3} (\bar{u}_i^s)^2 - \frac{8}{N_1 N_2 N_3} \cdot \sum_{p=1}^{N_1/2} \sum_{g=1}^{N_2/2} \sum_{r=1}^{N_3/2} (\bar{u}_i^l)^2 \\ Y^u &= \frac{1}{N_1 N_2 N_3} \cdot \sum_{n=1}^{N_1} \sum_{m=1}^{N_2} \sum_{q=1}^{N_3} (-2(\Delta_s)^2 (2S_{ij}^s S_{ij}^s)^{\frac{1}{2}} S_{ij}^s) - \\ & \quad - \frac{8}{N_1 N_2 N_3} \cdot \sum_{p=1}^{N_1/2} \sum_{g=1}^{N_2/2} \sum_{r=1}^{N_3/2} (-2(\Delta_l)^2 (2S_{ij}^l S_{ij}^l)^{\frac{1}{2}} S_{ij}^l). \end{aligned}$$

The condition for achieving the minimum is

$$\frac{\partial F^u}{\partial C_s} = -2(Z^u - Y^u \cdot C_s) \cdot Y^u = 0.$$

Thus, $Z^u - Y^u \cdot C_s = 0$.

With a certain time step $Tstep$, the empirical coefficient of the viscosity model is calculated by the following formula $C_s = Z^u / Y^u$, with $Tstep = 10 \cdot \tau$, τ is the time step.

4. Method to calculate the small-scale magnetic field

Here the same grid is used, which was used to calculate the small-scale turbulence coefficient, which deals with a grid twice the size of the cells along each axis.

The average values of the magnetic field strength H_1^2, H_2^2, H_3^2 for the total volume of the calculated area of the liquid flow are marked as $\langle H_1^2 \rangle, \langle H_2^2 \rangle, \langle H_3^2 \rangle$. These values can be calculated using smaller and larger calculation grids:

$$\langle H_i^2 \rangle = \frac{1}{N_1 N_2 N_3} \cdot \sum_{n=1}^{N_1} \sum_{m=1}^{N_2} \sum_{q=1}^{N_3} [(\overline{H}_i)^2 + (H'_i)^2] \quad (6)$$

where $(\overline{H}_i)^2 = \overline{H}_i \overline{H}_i$ and $(H'_i)^2 = \overline{H'_i} \overline{H'_i}$.

The magnetic subgrid-scale tensor for the smaller cells is

$$\tau_{ij}^H = \overline{H'_i H'_j} = -2D_s \cdot \Delta_s^2 \cdot (2 \cdot \overline{J}_{ij}^s \cdot \overline{J}_{ij}^s)^{\frac{1}{2}} \cdot \overline{J}_{ij}^s \quad (7)$$

The magnetic rotation tensor calculated in the smaller cells is $\overline{J}_{ij}^s = \frac{1}{2} \left(\frac{\partial \overline{H}_i^s}{\partial x_j} - \frac{\partial \overline{H}_j^s}{\partial x_i} \right)$,

where $n = \overline{1, N_1}$, $m = \overline{1, N_2}$, $q = \overline{1, N_3}$.

By substituting expression (7) into Eq. (6), we can obtain the average velocity value calculated in the smaller cells:

$$\langle H_i^2 \rangle^s = \frac{1}{N_1 N_2 N_3} \cdot \sum_{n=1}^{N_1} \sum_{m=1}^{N_2} \sum_{q=1}^{N_3} \left[(\overline{H}_i^s)^2 - 2 \cdot D_s \cdot \Delta_s^2 \cdot (2 \cdot \overline{J}_{ij}^s \cdot \overline{J}_{ij}^s)^{\frac{1}{2}} \overline{J}_{ij}^s \right] \quad (8)$$

The average value of the magnetic field strength calculated in the larger cells is

$$\langle H_i^2 \rangle^l = \frac{8}{N_1 N_2 N_3} \cdot \sum_{p=1}^{N_1/2} \sum_{g=1}^{N_2/2} \sum_{r=1}^{N_3/2} \left[(\overline{H}_i^l)^2 - 2 \cdot D_s \cdot \Delta_l^2 \cdot (2 \cdot \overline{J}_{ij}^l \cdot \overline{J}_{ij}^l)^{\frac{1}{2}} \overline{J}_{ij}^l \right] \quad (9)$$

The magnetic rotation tensor calculated in the larger cells is

$$\bar{J}_{ij}^l = \frac{1}{2} \left(\frac{\partial \bar{H}_i^l}{\partial x_j} - \frac{\partial \bar{H}_j^l}{\partial x_i} \right),$$

where $p = 1, 2, 3, \dots, N_1/2$, $g = 1, 2, 3, \dots, N_2/2$, $r = 1, 2, 3, \dots, N_3/2$.

$$\bar{H}_i^l(p, g, r) = \frac{1}{8} \left[\begin{aligned} &\bar{H}_i^s(2p-1, 2g-1, 2r-1) + \bar{H}_i^s(2p-1, 2g, 2r-1) + \\ &\bar{H}_i^s(2p-1, 2g, 2r) + \bar{H}_i^s(2p-1, 2g-1, 2r) + \\ &\bar{H}_i^s(2p, 2g-1, 2r-1) + \bar{H}_i^s(2p, 2g, 2r-1) + \\ &\bar{H}_i^s(2p, 2g, 2r) + \bar{H}_i^s(2p, 2g-1, 2r) \end{aligned} \right];$$

We introduce the following notation:

$$F^H = \left(\langle H_1^2 \rangle^s + \langle H_2^2 \rangle^s + \langle H_3^2 \rangle^s - \langle H_1^2 \rangle^l - \langle H_2^2 \rangle^l - \langle H_3^2 \rangle^l \right)^2$$

From equations (8) and (9) it yields

$$F^H = (Z^H - Y^H \cdot D_s)^2$$

where

$$\begin{aligned} Z^H &= \frac{1}{N_1 N_2 N_3} \cdot \sum_{n=1}^{N_1} \sum_{m=1}^{N_2} \sum_{q=1}^{N_3} (\bar{H}_i^2)^s - \frac{8}{N_1 N_2 N_3} \cdot \sum_{p=1}^{N_1/2} \sum_{g=1}^{N_2/2} \sum_{r=1}^{N_3/2} (\bar{H}_i^2)^l \\ Y^H &= \frac{1}{N_1 N_2 N_3} \cdot \sum_{n=1}^{N_1} \sum_{m=1}^{N_2} \sum_{q=1}^{N_3} (-2(\Delta_s)^2 (2J_{ij}^s J_{ij}^s)^{\frac{1}{2}} J_{ij}^s) - \\ &\quad - \frac{8}{N_1 N_2 N_3} \cdot \sum_{p=1}^{N_1/2} \sum_{g=1}^{N_2/2} \sum_{r=1}^{N_3/2} (-2(\Delta_l)^2 (2J_{ij}^l J_{ij}^l)^{\frac{1}{2}} J_{ij}^l). \end{aligned}$$

The condition for achieving the minimum is

$$\frac{\partial F^H}{\partial D_s} = -2(Z^H - Y^H \cdot D_s) \cdot Y^H = 0$$

Hence, $Z^H - Y^H \cdot D_s = 0$

Thus, the empirical coefficient of the viscosity model for the magnetic field at a certain time step $Tstep$ assumes the following form: $D_s = Z^H / Y^H$.

5. Numerical method

To solve the problem of homogeneous incompressible MHD turbulence, a scheme of splitting by physical parameters is used. The following physical interpretation of the splitting diagram is suggested. At the first stage, the Navier–Stokes equation is solved with no pressure

consideration. For the approximation of convective and diffusion equation members, a compact scheme of an increased order of accuracy is used [11]. At the second stage, the Poisson equation is solved, which is derived from the continuity equation by considering the velocity fields of the first stage. For the 3D Poisson equation, an original solution algorithm has been developed: a spectral transform in combination with the matrix run. At the third stage, the obtained pressure field is used to recalculate the final velocity field. At the fourth stage, the obtained velocity field is used to solve an equation in order to obtain the components of the magnetic field strength, which are included in the initial equation.

6. Algorithm to solve the equation of magnetic field strength

Let us consider Eq. (1) as the first component of the magnetic field strength:

$$\begin{aligned} \frac{\partial H_1}{\partial t} + \frac{1}{\text{Re}_m} \frac{\partial^2 H_1}{\partial x_1^2} + \frac{\partial}{\partial x_2} (u_2 H_1 - H_2 u_1) - \frac{1}{\text{Re}_m} \frac{\partial^2 H_1}{\partial x_2^2} + \\ + \frac{\partial}{\partial x_3} (u_3 H_1 - H_3 u_1) - \frac{1}{\text{Re}_m} \frac{\partial^2 H_1}{\partial x_3^2} = - \left(\frac{\partial \tau_{11}^H}{\partial x_1} + \frac{\partial \tau_{12}^H}{\partial x_2} + \frac{\partial \tau_{13}^H}{\partial x_3} \right). \end{aligned} \quad (10)$$

The strength of the magnetic field is found using the fractional step method. A run method is used at each stage of the fractional step method, i.e. a step-by step definition of the magnetic field strength values.

At the first stage, the magnetic field strength $H_1^{n+\frac{1}{3}}$ is found in the direction of the coordinate x_1 :

$$\frac{H_{li,j,k}^{n+\frac{1}{3}} - H_{li,j,k}^n}{\tau} = \frac{1}{2} \left[\Lambda_1 H_{li,j,k}^{n+\frac{1}{3}} + \Lambda_1 H_{li,j,k}^n \right] + \Lambda_2 H_{li,j,k}^n + \Lambda_3 H_{li,j,k}^n + f_{li,j,k}^n. \quad (11)$$

The operator $\Lambda_1 H_1$ is

$$\Lambda_1 H_1 = \frac{1}{\text{Re}_m} \frac{\partial^2 H_1}{\partial x_1^2} + \frac{\partial}{\partial x_1} (-\tau_{11}^H),$$

where the viscosity model and the magnetic rotation tensor are, respectively,

$$\tau_{11}^H = -2\eta_t \cdot J_{11},$$

$$J_{11} = \frac{1}{2} \left(\frac{\partial H_1}{\partial x_1} - \frac{\partial H_1}{\partial x_1} \right) = 0.$$

Similarly, the operator $\Lambda_2 H_1$ is

$$\Lambda_2 H_1 = -\frac{\partial}{\partial x_2} (u_2 H_1) + \frac{1}{\text{Re}_m} \frac{\partial^2 H_1}{\partial x_2^2} + \frac{\partial}{\partial x_2} (-\tau_{12}^H),$$

$$\tau_{12}^H = -2\eta_t \cdot J_{12},$$

$$J_{12} = \frac{1}{2} \left(\frac{\partial H_1}{\partial x_2} - \frac{\partial H_2}{\partial x_1} \right).$$

For the operator $\Lambda_3 H_1$,

$$\Lambda_3 H_1 = -\frac{\partial}{\partial x_3} (u_3 H_1) + \frac{1}{\text{Re}_m} \frac{\partial^2 H_1}{\partial x_3^2} + \frac{\partial}{\partial x_3} (-\tau_{13}^H),$$

$$\tau_{13}^H = -2\eta_t \cdot J_{13},$$

$$J_{13} = \frac{1}{2} \left(\frac{\partial H_1}{\partial x_3} - \frac{\partial H_3}{\partial x_1} \right),$$

$$f_1 = \frac{\partial}{\partial x_2} (H_2 u_1) + \frac{\partial}{\partial x_3} (H_3 u_1)$$

Writing the operator $\Lambda_1 H_1$ in the finite difference form,

$$\frac{\partial^2 H_1}{\partial x_1^2} = \frac{(H_1)_{i+1,j,k} - 2(H_1)_{i,j,k} - (H_1)_{i-1,j,k}}{\Delta x_1^2},$$

(12)

$$\frac{\partial}{\partial x_1} (-\tau_{11}^H) = 0,$$

are determined as a convective member for the operator $\Lambda_2 H_1$ on a staggered grid as

$$\frac{\partial (u_2 H_1)}{\partial x_2} = \frac{A_y \cdot ((H_1)_{i,j+1,k} + (H_1)_{i,j,k}) - B_y ((H_1)_{i,j,k} + (H_1)_{i,j-1,k})}{2\Delta x_2},$$

where $A_y = (u_2)_{i,j+\frac{1}{2},k}$ and $B_y = (u_2)_{i,j-\frac{1}{2},k}$.

Similarly, the diffusion member for the operator $\Lambda_2 H_1$ is

$$\frac{\partial^2 H_1}{\partial x_2^2} = \frac{(H_1)_{i,j+1,k} - 2(H_1)_{i,j,k} + (H_1)_{i,j-1,k}}{2\Delta x_2^2},$$

(13)

In addition, a strength tensor is determined for the operator $\Lambda_2 H_1$:

$$\begin{aligned} \frac{\partial}{\partial x_2}(-\tau_{21}^H) &= \frac{\partial}{\partial x_2}(2\eta_t \cdot J_{12}) = \\ &= \frac{2}{2 \cdot \Delta x_2} \left[(\eta_t)_{i,j+\frac{1}{2},k} \cdot \left[\frac{(H_1)_{i,j+1,k} - (H_1)_{i,j,k}}{\Delta x_2} - \frac{(H_2)_{i+1,j,k} - (H_2)_{i,j,k}}{\Delta x_1} \right] - \right. \\ &\quad \left. - (\eta_t)_{i,j-\frac{1}{2},k} \cdot \left[\frac{(H_1)_{i,j,k} - (H_1)_{i,j-1,k}}{\Delta x_2} - \frac{(H_2)_{i,j,k} - (H_2)_{i-1,j,k}}{\Delta x_1} \right] \right] \end{aligned}$$

Similarly, the operator $\Lambda_3 H_1$ is determined and, correspondingly, the convective term is

$$\frac{\partial(u_3 H_1)}{\partial x_3} = \frac{A_z \cdot ((H_1)_{i,j,k+1} + (H_1)_{i,j,k}) - B_z \cdot ((H_1)_{i,j,k} + (H_1)_{i,j-1,k})}{2\Delta x_3} \quad (14)$$

where $A_z = (u_3)_{i,j,k+\frac{1}{2}}$, $B_z = (u_3)_{i,j,k-\frac{1}{2}}$

The diffusion member for the operator $\Lambda_3 H_1$ is

$$\frac{\partial^2 H_1}{\partial x_3^2} = \frac{(H_1)_{i,j,k+1} - 2(H_1)_{i,j,k} + (H_1)_{i,j,k-1}}{2\Delta x_3^2}$$

and the strength tensor is

$$\begin{aligned} \frac{\partial}{\partial x_3}(-\tau_{13}^H) &= \frac{\partial}{\partial x_3}(2\eta_t \cdot J_{13}) = \\ &= \frac{2}{2 \cdot \Delta x_3} \left[(\eta_t)_{i,j,k+\frac{1}{2}} \cdot \left[\frac{(H_1)_{i,j,k+1} - (H_1)_{i,j,k}}{\Delta x_3} - \frac{(H_3)_{i+1,j,k} - (H_3)_{i,j,k}}{\Delta x_1} \right] - \right. \\ &\quad \left. - (\eta_t)_{i,j,k-\frac{1}{2}} \cdot \left[\frac{(H_1)_{i,j,k} - (H_1)_{i,j,k-1}}{\Delta x_3} - \frac{(H_3)_{i,j,k} - (H_3)_{i-1,j,k}}{\Delta x_1} \right] \right], \end{aligned}$$

As a result, we have

$$\begin{aligned} \frac{(H_1)_{i,j,k}^{n+\frac{1}{3}} + (H_1)_{i,j,k}^n}{\tau} &= \frac{1}{2} \left[\frac{1}{\text{Re}_m} \frac{(H_1)_{i+1,j,k}^{n+\frac{1}{3}} - 2(H_1)_{i,j,k}^{n+\frac{1}{3}} + (H_1)_{i-1,j,k}^{n+\frac{1}{3}}}{\Delta x_1^2} + \Lambda_1 (H_1)_{i,j,k}^n \right] + \\ &+ \Lambda_2 (H_1)_{i,j,k}^n + \Lambda_3 (H_1)_{i,j,k}^n + (f_1)_{i,j,k}. \end{aligned} \quad (15)$$

The equation is solved by the run method and found to be $(H_1)_{i,j,k}^{n+\frac{1}{3}}$. The $(H_1)_{i,j,k}^{n+\frac{2}{3}}$ and $(H_1)_{i,j,k}^{n+1}$ components of the magnetic field strength are defined in a similar way. Thus, all the components of the magnetic field strength have been determined in this way.

7. Numerical modelling results

The numerical model allowed to describe the homogeneous magneto hydrodynamic turbulence decay based on large eddy simulation. For this task, the kinematic viscosity $\nu = 10^{-4}$ was taken constant and the magnetic Reynolds number was set in the range $Re_m = 10^3 \div 10^4$. The characteristic values of the velocity, length, and magnetic field strength were taken equal to $U_{char} = 1, L_{char} = 1, H_{char} = 1$, respectively. The Alfvén number, characterizing the motion of conductive fluid for various magnetic Reynolds numbers, was $A = Ha^2 / Re_m \cdot Re$, where the Hartmann number was $Ha = 1$.

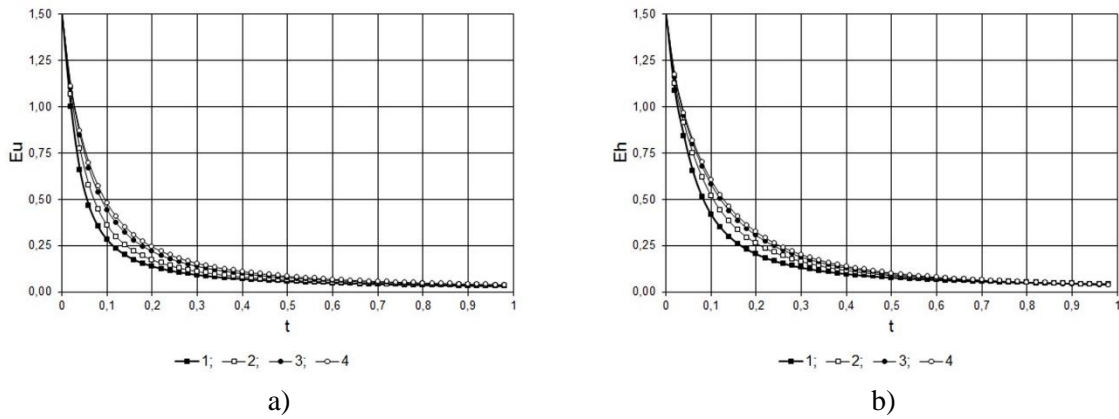


Figure 1: Variation of a) kinetic turbulent energy b) magnetic energy vs. magnetic Reynolds numbers at different points in time: 1) $Re_m = 10^3$; 2) $Re_m = 2 \cdot 10^3$; 3) $Re_m = 5 \cdot 10^3$; 4) $Re_m = 10^4$.

For the calculations, the grid $128 \times 128 \times 128$ was used. The time step was taken equal to $\Delta\tau = 0.001$. As a result of the simulation with different magnetic Reynolds numbers, the following turbulence characteristics were obtained: kinetic energy, magnetic energy, integral scale, Taylor scale, transverse and longitudinal correlation functions. The results displayed in Fig. 1 shows the decay of kinetic and magnetic energies calculated at different magnetic Reynolds numbers. Figs. 1 shows the dynamics of the mutual influence of magnetic and kinetic energies at different time instants: at the initial time, the kinetic and magnetic energies were given the same; at the next instant when a fluid with high conductivity was studied. The decay of MHD turbulence occurred faster than when Re_m started to rise, which specifies a fluid with smaller conductivity, and at $Re_m = 10^4$ the decay of MHD turbulence practically corresponded to the decay of isotropic turbulence [12].

According to the semi-empirical theory of turbulence, the integral scale must grow with time. The results presented in Fig. 2a illustrates the effect of magnetic Reynolds number on the internal structure of MHD turbulence. A variation of the coefficient of magnetic viscosity leads to a proportional change in integral scale. Fig.2a shows that the size of large eddies rapidly increases at a small magnetic Reynolds number $Re_m = 10^3$ than in the case, when $Re_m = 10^4$, which leads to fast energy dissipation. Fig. 2b shows the change of the Taylor microscale at different magnetic Reynolds numbers. It can be seen in the case with $Re_m = 10^3$ when the magnetic Reynolds number is large, the dissipation rate increases. In the case $Re_m = 10^4$ when the magnetic Reynolds number is smaller, the scale gradually increases, and the small-scale structure of turbulence tends to slow isotropy. This also

indicates that with small Re_m numbers the decay of isotropic turbulence occurs faster than in the case when Re_m is high.

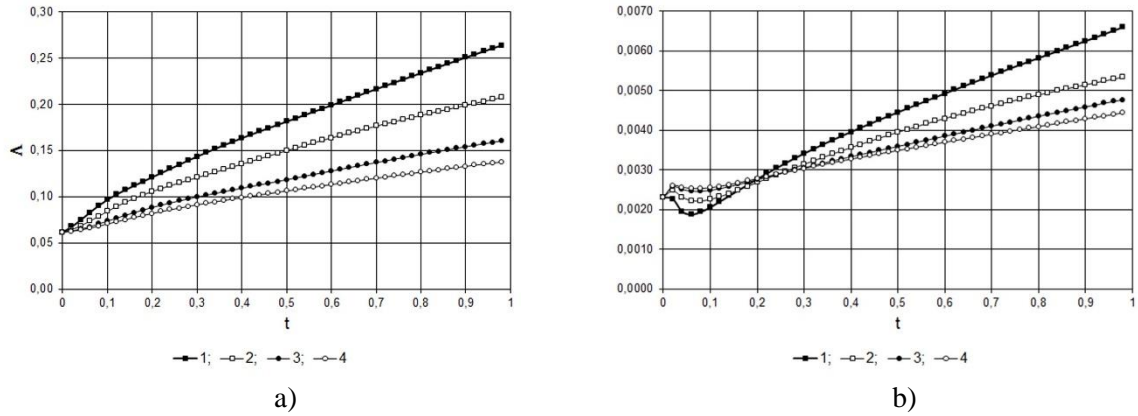


Figure 2: Change of the a) integral turbulence scale and b) Taylor scale calculated at different magnetic Reynolds numbers at different points in time: 1) $Re_m = 10^3$; 2) $Re_m = 2 \cdot 10^3$; 3) $Re_m = 5 \cdot 10^3$; 4) $Re_m = 10^4$.

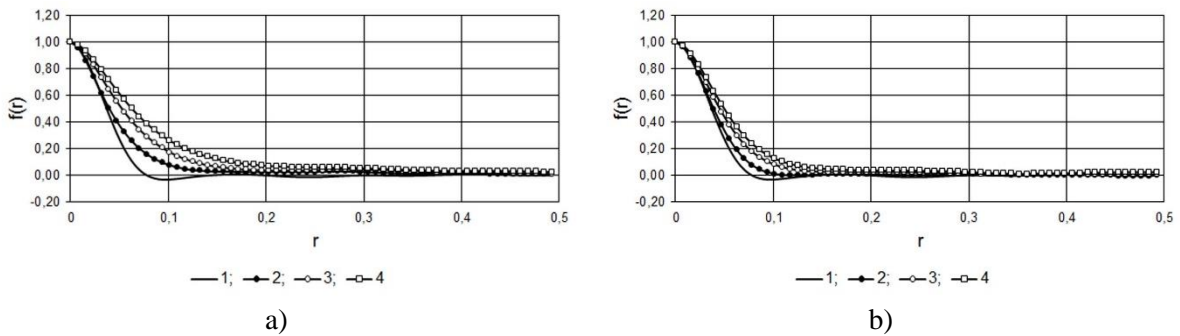


Figure 3: Change of the longitudinal correlation function $f(r)$ when (a) $Re_m = 10^3$ and (b) $Re_m = 10^4$ at different points in time: 1) $t = 0.1$; 2) $t = 0.2$; 3) $t = 0.3$; 4) $t = 0.5$.

The correlation function expresses an averaged by volume correlation ratio between the velocity components at various points: the farther points are located between different components of the velocity, the smaller ones should be the correlation coefficients, i.e. they should be close to zero. Fig. 3a shows the change in longitudinal correlation function $f(r)$ in time calculated at $Re_m = 10^4$ and $Re_m = 10^3$. It is seen that, when being increased, the function value r tends to zero. The character of the correlation change corresponds to the change of the correlation functions given in [13].

8. Conclusions

Based on the LES method, the influence of magnetic Reynolds number on the decay of uniform magnetohydrodynamic turbulence has been numerically modelled. The obtained results allow to sufficiently accurately calculate the variations of the characteristics of uniform MHD turbulence with time at large magnetic Reynolds numbers. A numerical algorithm has been developed to solve unsteady three-dimensional magnetohydrodynamic equations as well as to model the MHD turbulence decay at different magnetic Reynolds numbers.

A numerical algorithm has been developed to solve unsteady three-dimensional magnetohydrodynamic equations as well as to model the MHD turbulence decay at different magnetic Reynolds numbers. Physical processes and phenomena of uniform MHD turbulence were identified in the numerical simulation.

References

1. G.K. Batchelor. On the spontaneous magnetic field in a conducting liquid in turbulent motion. *Proc. Roy. Soc. A*201, 16, 405–416, 1950.
2. U. Schumann. Numerical simulation of the transition from three- to two-dimensional turbulence under a uniform magnetic field. *J. Fluid Mech.*, 74, pp. 31–58, 1976.
3. P. Burattini, O. Zikanov, B. Knaepen. Decay of magnetohydrodynamic turbulence at low magnetic Reynolds number. *J. Fluid Mech.*, 657, pp. 502–538, 2010.
4. B. Knaepen, S. Kassinos and D. Carati. Magnetohydrodynamic turbulence at moderate magnetic Reynolds number. *J. Fluid Mech.*, 513, no. 3, pp. 199–220, 2004.
5. B. Knaepen, P. Moin. Large-eddy simulation of conductive flows at low magnetic Reynolds number. *Physics of Fluids*, 15, pp. 297–306, 2003
6. B.Knaepen, S.Kassinos and D.Carati. Magnetohydrodynamic turbulence at moderate magnetic Reynolds number. *J. Fluid Mech.*, vol. 513 (2004), no. 3, pp. 199–220.
7. O. Vorobev, A. Zikanov. Davidson and B. Knaepen. Anisotropy of magnetohydrodynamic turbulence at low magnetic Reynolds number. *J. Physics of fluids*, 17, pp. 4–11, 2005.
8. G.Sahoo, P.Perlekar, R.Panditn. Systematics of the magnetic Prandtl-number dependence of homogeneous, isotropic magnetohydrodynamic turbulence. *New J. Phys.*, 13, pp. 1367–2630, 2011.
9. V.M. Ievlev. The Method of Fractional Steps for Solution of Problems of Mathematical Physics. *Nauka*, 1975.
10. B. T. Zhumagulov, D. B. Zhakebayev, and A. U. Abdibekova. The decay of MHD turbulence depending on the conductive properties of the environment. *Magnetohydrodynamics*, 50, No. 2, 2014.
11. U.S. Abdibekov, B. T. Zhumagulov, D. B. Zhakebayev, K. Zh. Zhubat. Simulation of isotropic turbulence degeneration based on the large-eddy method. *Mathematical Models and Computer Simulations*, 5, No. 4, pp. 360–370, 2013.
12. U.S. Abdibekov, D. B. Zhakebayev. Modelling of the decay of isotropic turbulence by LES. *Journal of Physics: Conference Series*, Proceedings of the 13th European turbulence conference, Warsaw, 318, pp.327–338, 2011.
13. N. de Divitiis, Lyapunov analysis for fully developed homogeneous isotropic turbulence. *Theor. Comput. Fluid Dyn.* 25, No. 6, pp. 421–445, 2011.

Cover illustration: *THMT from micro to macro scales: SGS heat flux in hydrogen-air premixed flame* (from Hiraoka et al., p. 501); *pollutant clouds in downtown Sarajevo during winter inversion with a mild wind (URANS, from Kenjereš et al. p. 719).*

Turbulence, Heat and Mass Transfer 8

Proceedings of the Eight International Symposium on Turbulence, Heat and Mass Transfer, Sarajevo, Bosnia and Herzegovina, September 15-18 2015/ K. Hanjalić, T. Miyauchi, D. Borello, M. Hadžiabdić, P. Venturini (Editors); Begell House Inc.

ISSN 2377-2816 (Online);

ISSN 2377-4169 (CD-ROM)

ISBN: 978-1-56700-427-4 (Online)

ISBN: 978-1-56700-428-8 (CD-ROM)

Copyright © 2015 by Begell House Inc./ICHMT. All rights reserved.

Neither this book nor any part may be reproduced or transmitted in any form by any means, electronic or mechanical, including photocopying, microfilming and recording, or by any information storage and retrieval system, without permission in writing from the publisher.

Begell House Inc.'s consent does not extend to copying for general distribution, for promotion, for creating new work, or for resale. Specific permission must be obtained in writing from Begell House for such copying.

Detailed all inquiries to Begell House Inc., 50 Cross Highway, Redding, CT 06896, USA

Printed in Sarajevo, Bosnia and Herzegovina.